Limitations on the stabilization of resistive tearing modes

T. A. Gianakon[a)]
Los Alamos National Laboratory, Los Alamos, New Mexico 87505

(Received 17 April 2001; accepted 19 June 2001)

A study of the passive stabilization of resistive magnetohydrodynamic (MHD) tearing modes is presented in the context of zero β full-MHD equations with the NIMROD [A. H. Glasser *et al.*, Plasma Phys. Controlled Fusion **41**, A747 (1999)] code. The stabilization effect of the current is modeled by a source term in the Ohm's law. This source term is evaluated based on a diffusive model with anisotropic diffusivities parallel and perpendicular to the perturbed magnetic field lines and driven by a spatially localized source. The effects of spatial localization of the current source are explored that illustrate stabilization down to a combination of source current channel width and parallel and perpendicular diffusion scale lengths. *© 2001 American Institute of Physics.*
[DOI: 10.1063/1.1391447]

I. INTRODUCTION

The performance gains of the last several years in tokamak fusion plasmas has generated a resurgence in the observation of low helicity magnetic oscillations.[1,2] Often, the onset of such oscillations either cause a violent plasma disruption[3,4] or significantly degrade the plasma confinement.[1] Experimental observations indicate that these instabilities are associated with magnetic reconnection—an interpretation based on the observation of the slow growth of these instabilities, mode numbers which are resonant in the plasma, and the presence of flat spots in the electron temperature profile about these resonant surfaces.[1,2] Often these observations are interpreted based on a combination of standard resistive magnetohydrodynamics (MHD) (Δ' tearing modes) and/or destabilization from the perturbed bootstrap current (neoclassical tearing modes or NTM).[5–7]

Theoretical interpretations have projected that these modes will be problematic for fusion reactor concepts in general that have significant bootstrap currents in regions of nonreversed magnetic shear.[8,9] Subsequently, various authors have proposed that phased and passive current drive in the presence of rotation could be applied to stabilize the offending tearing modes[10–18] and recent experimental work demonstrates that passive stabilization is feasible.[19] The approach in these theoretical analyses is to add an auxiliary current source to the Ohm's law and then following a standard Rutherford analysis[20] to develop an evolution equation for the island width. The typical evolution equation for the island width W is expressed as

$$\frac{\mu_0}{\eta}\frac{dW}{dt}=\Delta'+\Delta'_{\rm rf}+\Delta'_{\rm nc}+\cdots, \qquad (1)$$

where Δ' is the contribution from resistive MHD, $\Delta'_{\rm nc}$ is a neoclassical contribution[5,21] and $\Delta'_{\rm rf}$ is the contribution from the rf induced currents,[11,22] and additional effects may exist.[8,21] The radial, poloidal, and toroidal profile of this current source is then tailored to provide a current, and also then a perturbed magnetic field, to cancel the magnetic perturbation of the instability, which in terms of the island evolution equation makes $\Delta'_{\rm rf}$ sufficiently large and negative to overcome the other contributions in the island evolution equation. The $\Delta'_{\rm rf}$ has previously been shown to be significantly reduced[11,12] when the island width becomes smaller than the width of the current being deposited, so that the minimum island width for stabilization is expected to be limited by this value.

Complete stabilization of the NTM has been predicted provided that the current channel can be made smaller than the nonlinear threshold for instability associated with the neoclassical tearing mode. The most restrictive threshold mechanism for the neoclassical tearing mode is caused by insufficient flattening of the pressure gradient in the vicinity of the island due to finite parallel transport effects. The typical scale length W_d at which this effect is important can be estimated based on balancing transit times across the island half width for cross-field diffusion, $\tau_\perp=(W_d/2)^2/\chi_\perp$, with parallel-diffusion, $\tau_\parallel=1/k_\parallel^2\chi_\parallel$, where $k_\parallel$ is the parallel wave number.[23] The diffusion of an rf induced current about an island is expected to be limited in much the same way the neoclassical tearing mode has a threshold from anisotropic thermal diffusion. The focus of this paper will be directed at investigating through numerical simulations the extent to which the current channel associated with the rf and the anisotropic current diffusion play a role in limiting the extent of the stabilized island width. Extensive simulation work that gave preliminary consideration to the W_d effect associated with the stabilization of the neoclassical tearing mode have been made.[22] The principal limitation of that work was that they did not access island widths smaller than that set by the neoclassical tearing mode threshold and appear to be in a mode that is limited by the magnitude of the current and not the current channel width. Though the effect does appear to be present in some of the simulation results. (See Fig. 7 of Ref. 22.) The effect can be better isolated by investigation of a resistive tearing mode, e.g., $\Delta'_{\rm nc}=0$ and $\Delta'>0$, that in the

[a)]Electronic mail: gianakon@lanl.gov

context of MHD will be robustly unstable even at vanishingly small island width.

The implementation of such an auxiliary current drive is a deceptively simple addition to the Ohm's law, but in principal is a challenge to calculate. Nominally, a full time-dependent kinetic expression in three dimensional geometry should be solved, but such calculations are prohibitively expensive. Alternatively, the problem can be decomposed into one of two simpler problems either (1) by handling island geometry/MHD aspects with island evolution equations and focusing computational resources on the dynamics of the rf with a kinetic simulation as detailed in Ref. 12 or, as detailed in this paper, (2) by simplifying the rf dynamics with a low order moment of the kinetic equation and focusing computational resources on solving MHD equations. The limitation of the first approach is that the small island width dynamics can only be implemented based on a preassumption of the expected behavior. This paper seeks to study this particular limit.

The simple stabilization picture suggested by Eq. (1) could be further complicated by several features in an actual device: mode amplitude and phase detection especially in the presence of rotation, relative phasing of the rf induced current that determines the sign of Δ'_{rf}, and the finite time response of the rf induced current. With the exception of rotation effects, these effects are mainly relevant for active stabilization schemes where the rf induced current is effectively turned on and off relative to some position of the island O-point. (Reference 24 contains a discussion of feedback control issues in a slightly different context but is relevant to active stabilization schemes.) The simulations presented here will have this character in that the auxiliary current is statically phased to the island O-point. These results will then be extended through a simple island evolution equation to the experimentally successful passive stabilization scheme,[22] in which the rf is always on at the offending resonant surface, but mode rotation causes the induced current to alternate between stabilizing and destabilizing contributions subject to the limiting effects at small island width.

To facilitate this discussion, the model equations as implemented in the NIMROD code are presented in Sec. II along with a model of the auxiliary current. In Sec. III, initial value simulations which study the stabilization of a standard resistive (Δ') instability are presented and interpreted in terms of an island evolution equation. The island evolution equation is then extended to include rotation effects. Conclusions are discussed in Sec. IV.

II. MODEL

The NIMROD[25] code is a nonlinear, initial value code that solves solves the full-MHD equations. The zero-β MHD equations considered here consist of the single fluid momentum equation

$$\rho \frac{\partial \vec{v}}{\partial t} + \rho \vec{v} \cdot \nabla \vec{v} = \vec{J} \times \vec{B} - \nu \nabla^2 \vec{v}, \tag{2}$$

and the combination of Faraday's law and Ohm's law,

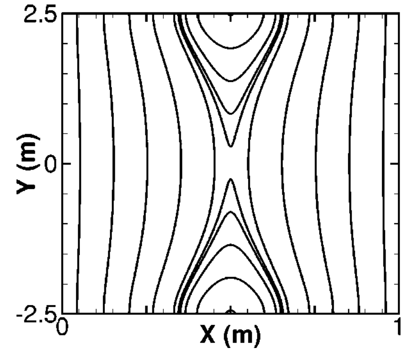

FIG. 1. Slab geometry has a width of 1 (m), height of 5 (m), and a periodic length of 2π. Also illustrated are stream traces of the magnetic field illustrating the initial island width for the simulation. A finite element mesh of $mx = 80$ by $my = 80$ with a polynomial degree of three has been used.

$$\frac{\partial \vec{B}}{\partial t} = -\nabla \times \{ -\vec{v} \times \vec{B} + \eta \vec{J} + \eta_{\mathrm{rf}} J_{\mathrm{rf}} \nabla z \}, \tag{3}$$

where $\vec{v}$ is the single fluid velocity, $\vec{B}$ is the magnetic field, $\mu_0 \vec{J} = \nabla \times \vec{B}$ is the plasma current, ν is the kinematic viscosity, η is the plasma resistivity, η_{rf} is the effective resistivity associated with the rf term, J_{rf} is an rf induced current source that has a separate evolution equation discussed in the following paragraph, ρ is plasma density, and t is time. All units follow the convention of the NIMROD code which is in SI units.

The slab geometry of the simulations is periodic in the y-direction and bounded by conducting walls at $x = 0$ and $x = 1$ (m) (see Fig. 1). A Fourier expansion is used in the periodic z direction and cubic, finite elements in the other two directions. This slab geometry and the equilibrium magnetic fields and current profiles illustrated in Fig. 2 were previously used in a study of the resistive wall mode.[26] A $k_z = 0$ resonant condition is present at $X = 0.5$ that allows for the formation of a magnetic island. A self-consistent island, in the absence of the rf term is allowed to evolve and is used as an initial condition in this stabilization study. This initial island is illustrated by the magnetic-field line trace of Fig. 1. The island width is defined as the largest radial extant of the field-line traces that pass through the island X point. The initial condition has an island width of 0.312 (m). Uniform resistivity, viscosity, and density profiles are chosen with

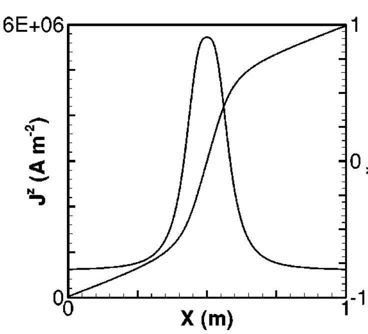

FIG. 2. The equilibrium field has a $B^z = 100(T)$ and a B^y which leads to a $kz = 0$ resonance condition. The current profile is peaked about the resonant surface.

$\eta/\mu_0 = 10^3$, $\nu/\mu_0 = 10^4$, and $n = 0.951\,75(10^{19})$ such that $S = 5(10^5)$ and $\mathrm{Pr} = 10$. The NIMROD code has successfully run the MHD portion of the instability nonlinearly with $S = 5(10^7)$ with little difficulty. The simulations with the auxiliary current, except for a few select cases run at higher S that are not presented here, are all conducted at $S = 5(10^5)$. The principal advantage is the shorter compute time of the nonlinear simulations allows a broader parameter scan.

A simplified current drive model for J_{rf} can be derived based on a separation between fast and thermal electron species. Such an equation for J_{rf} can be developed by considering the parallel velocity moment of the electron kinetic equation,[27,28]

$$\frac{\partial f}{\partial t} + \frac{v_\parallel}{B}\vec{B}\cdot\nabla f - \frac{e}{m}E_\parallel \frac{\partial f}{\partial v_\parallel} = C(f) + \frac{\partial}{\partial \vec{v}}\cdot \vec{\vec{D}}_{\mathrm{rf}}\cdot \frac{\partial f}{\partial \vec{v}} + \chi_\perp \nabla^2 f, \tag{4}$$

where $E_\parallel$ is the parallel projection of the electric field, $C(f)$ is a standard collision operator, D_{rf} is a velocity-dependent diffusion operator that accounts for the effects of the rf on the particle distribution, and $\chi_\perp$ is a diffusion operator that effectively describes anomalous transport from microturbulence. If the parallel velocity moment of this equation is computed, then

$$\frac{\partial J_{\mathrm{rf}}^{\zeta}}{\partial t} = \frac{e}{m_e B}\vec{B}\cdot\nabla P_f - \nu_{\mathrm{rf}} J_{\mathrm{rf}}^{\zeta} - S_{\mathrm{rf}} + \chi_\perp \nabla^2 J_{\mathrm{rf}}^{\zeta} + E_\parallel n_f \frac{e^2}{m_e}, \tag{5}$$

where $n_{\mathrm{rf}} = \int d^3v\, f$, is the fast particle density and is presumed to be small; $J_{\mathrm{rf}} = -e n_{\mathrm{rf}} \int d^3 v v_\parallel f$ is the rf current density where either the ions are assumed to be fixed or the electrons are sufficiently energetic that the ion velocity may be neglected; $P_f = m_e \int d^3 v\, v_\parallel v_\parallel f$ is the fast particle pressure and a closure of the form $\vec{B}/B\cdot\nabla P_f = m_e/e\chi_\parallel \vec{B}\cdot\nabla(\vec{B}\cdot\nabla J_{\mathrm{rf}}^{\zeta}/B^2)$ is assumed.[22] The velocity integral over the rf diffusive operator and the collision operator have been replaced with $-\nu_{\mathrm{rf}} J_{\mathrm{rf}}^{\zeta} - S_{\mathrm{rf}}$, where S_{rf} is a specified source distribution[12] that could include the effects of collisional slowing of the fast electron population. This effect will be ignored. Furthermore, the term $E_\parallel n_{\mathrm{rf}}$ is dropped on the basis that the perturbation to the total density is small. As explained in Ref. 12, this term can be important when modeling the finite time response of rf generated currents. This assumption does not suggest the instantaneous generation of current in the Ohm's law. The equation for J_{rf} is implemented as follows:

$$\frac{\partial J_{\mathrm{rf}}}{\partial t} = \chi_\perp \nabla^2 J_{\mathrm{rf}} + \chi_\parallel \vec{B}\cdot\nabla\left(\frac{\vec{B}\cdot\nabla J_{\mathrm{rf}}}{B^2}\right) - S_{\mathrm{rf}}. \tag{6}$$

In the simulations that follow, the source term for this auxiliary current equation is spatially localized in the finite element plane as a square box that has width δ_x, height δ_y, is centered at (X_0, Y_0), and uniform magnitude S_{rf}. The perpendicular diffusion is set to $\chi_\perp = 10^3(\mathrm{m^2\,s^{-1}})$, which effectively puts the diffusion of the current source J_{rf} on a faster evolution timescale than the island dynamics. The parallel diffusion has typically been set to $\chi_\parallel = 10^{11}(\mathrm{m^2\,s^{-1}})$, but this study does consider a range of values between $10^8(\mathrm{m^2\,s^{-1}})$ and $10^{12}(\mathrm{m^2\,s^{-1}})$.

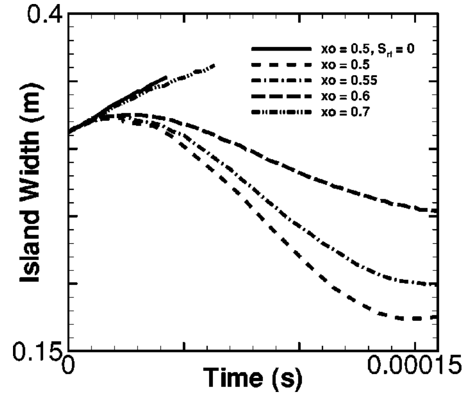

FIG. 3. An increase in the source offset reduces the stabilization effect of the rf induced current and the ultimate saturation width of the island. The source specifications are $\delta_x = 0.3$, $\delta_y = 1.0$, $S_{\mathrm{rf}} = 0.3333(10^{13})$, $\chi_\perp = 10^3\ \mathrm{m^2\,s^{-1}}$ and $\chi_\parallel = 10^{11}\ \mathrm{m^2\,s^{-1}}$. Here, $S = 5(10^5)$ and $\mathrm{Pr}_m = 10$.

III. RESULTS

A recognized feature of the stabilization process for the tearing mode is that a given current source that is localized exclusively inside the island separatrix can be stabilizing with the appropriate sign. The most efficient stabilization is a delta function source located exactly at the island O-point. The same current source localized outside the island separatrix is destabilizing, though not as strongly.[11] This effect is important for the passive stabilization scheme since in the presence of rotation, the localized auxiliary current drive can still provide net stabilization. This premise is tested in Fig. 3 with a source of finite size ($\delta_x, \delta_y = 0.3$) of fixed magnitude $S_{\mathrm{rf}} = 0.3333(10^{13})$ that is centered at several positions between the island O-point at $X_0 = 0.5$ and the initial separatrix across the O-point with $X = 0.66$. The optimum stabilization is seen for the centering at the O-point.

In Fig. 4, the time evolution of the island width for five

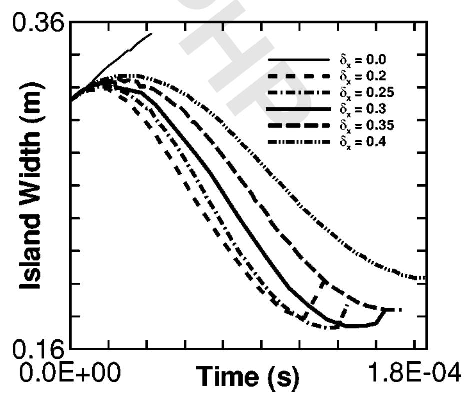

FIG. 4. The initial decay of the island width is weakly sensitive to the current channel width due to the fact that $\delta_x S_{\mathrm{rf}}$ is held constant, which optimizes the magnitude of the current at the O-point. The minimum island width is insensitive to the current channel width because of source diffusion effects. The source specifications are $\delta_y = 1.0$, $\delta_x S_{\mathrm{rf}} = 1.00(10^{12})$, $\chi_\perp = 10^3\ \mathrm{m^2\,s^{-1}}$ and $\chi_\parallel = 10^{11}\ \mathrm{m^2\,s^{-1}}$. Here, $S = 5(10^5)$ and $\mathrm{Pr}_m = 10$.

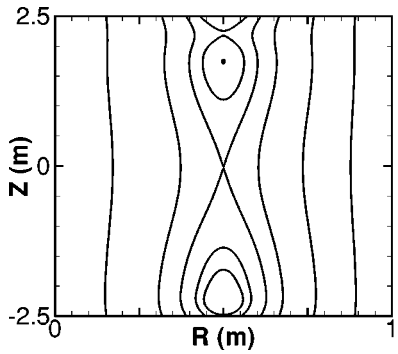

FIG. 5. The rf induced current at the initial island's O-point causes the formation of an X-point inside the island. This is an oppositely phased island that can eventually grow larger than the initial island and the configuration returns to instability.

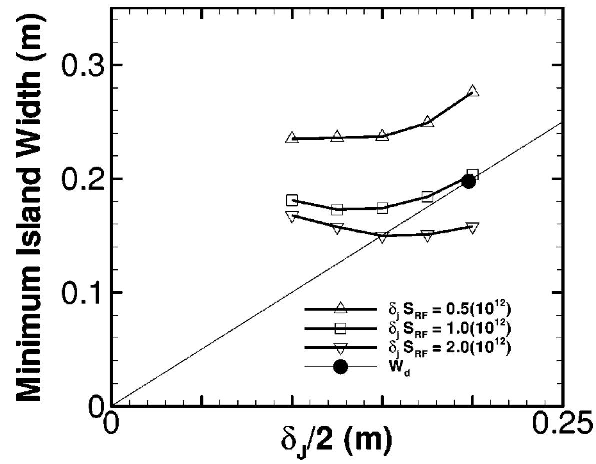

FIG. 6. The minimum island width $W_{\min}$ is limited by the anisotropic diffusion width W_d for a sufficiently strong current source. The source specifications are $\delta_y = 1.0$, $\chi_\perp = 10^3\,\mathrm{m^2\,s^{-1}}$, and $\chi_\parallel = 10^{11}\,\mathrm{m^2\,s^{-1}}$. Here, $S = 5(10^5)$ and $\mathrm{Pr}_m = 10$.

current channel widths is presented. The total driven current between each channel width is kept approximately constant by holding the product of the source magnitude and current channel width constant $\delta_J S_{\mathrm{rf}} = \mathrm{constant}$. A typical experiment usually has little flexibility in this regard since both are limited by initial construction details. As the magnitude of the current ramps up linearly throughout the evolution, the current perturbation is initially insufficient in magnitude to stabilize the tearing mode even though the current channel is smaller than the island width. Once the current reaches sufficient magnitude, stabilization begins which leads to a contraction of the island size. Once the island reaches a sufficiently small size either the island saturates or the island transitions back to instability. Whether the instability saturates or reverts back to instability is sensitive to what mechanism sets the minimum island width: the current channel width or an anisotropic diffusion width. The actual cause of the abrupt change is the result of a phase shifted island being driven by the rf current. Recall that the driven current perturbation is opposite in sign to the current perturbation associated with the tearing mode. An example of this phase shifted island and the generation of a secondary X-point inside the original island's O-point is illustrated in Fig. 5. When this phase shifted island is smaller than the original island contraction is observed, but once the phase shifted island is larger, then both the driven current perturbation and the tearing mode current perturbation have the same sign. This gives an additional increase to what would be the normal growth rate of the tearing mode that can be identified both by switching the sign of Δ'_{rf} in Eq. (1) or by noting the increase in slope at the transition point associated with the curves of Fig. 4. One possible recourse to this phase problem is to rotate the island X- and O-points past the rf source, which is a typical operating scenario for tokamaks that often have significant beam driven rotation. This will be discussed at the end of this chapter in terms of a modified island evolution equation.

In Fig. 6, the saturated or minimum island widths are presented for three power levels as functions of the current channel half-width. The current channel half-width is motivated on the physical grounds that this approximately marks the point where half the current generated would be outside the separatrix of the minimum island width. The minimum island width is observed to have a weak dependency on the current channel width in this particular figure. The weak dependency is because this set of simulations are limited not by the current channel, but by the anisotropic diffusion scale length, W_d. The anisotropic diffusion scale length is estimated based on balancing transit times across the island half-width for cross-field diffusion, $\tau_\perp = (W_d/2)^2/\chi_\perp$, with parallel-diffusion, $\tau_\parallel = 1/k_\parallel^2 \chi_\parallel$, where the parallel wave number is given by $k_\parallel \simeq 0.5 k_y W_d / B_0^Z (dB_0^y/dx)$. The equilibrium investigated here has $W_d = 19.8(\chi_\perp/\chi_\parallel)^{1/4}$. When an island is on the order of this width, diffusion processes are unaffected by the helical structure of the island and in this case the rf driven current no longer takes on a helical current perturbation necessary for stabilization and so only indirectly and weakly affects the stability of the tearing mode by adding to the equilibrium current. This affect is further discussed in the following paragraph. The magnitude of the driven current does play a role in determining whether the minimum island width saturates or whether the width approaches saturation but then transitions to the alternately phased unstable island. The island widths along the lowest power curve in Fig. 6 all saturate and the oppositely phased island never manifests but the higher power curves especially at the narrowest current channels are prone to this problem. The observation is made that for a sufficiently strong current source, the minimum island width is principally limited to W_d and when the island is driven to this width the phase instability becomes important.

To identify further that the anisotropic thermal diffusion length scale sets a limit on the minimum width, a scan versus W_d is presented in Fig. 7. In this figure, the current channel is held fixed while the magnitude of the parallel diffusion coefficient is varied. In particular, the observation is made that

$$W_{\min} = \begin{cases} W_d\,; \delta_J/2 < W_d\,, \\ \delta_J/2; \delta_J/2 > W_d\,. \end{cases} \tag{7}$$

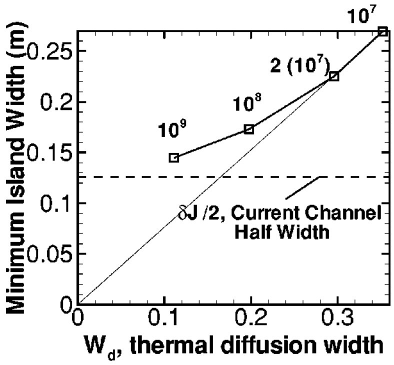

FIG. 7. The minimum island width $W_{\min}$ is determined by the current channel width δj and the thermal diffusion width W_d. The numbers beside each data point is the magnitude of $\chi_{\parallel}/\chi_{\perp}$ such that $W_d = 19.8(\chi_{\parallel}/\chi_{\perp})^{0.25}$. Here, $W_{\min} \simeq \delta_j$ when $\delta_j > W_d$ and $W_{\min} \simeq W_d$ when $\delta_j < W_d$.

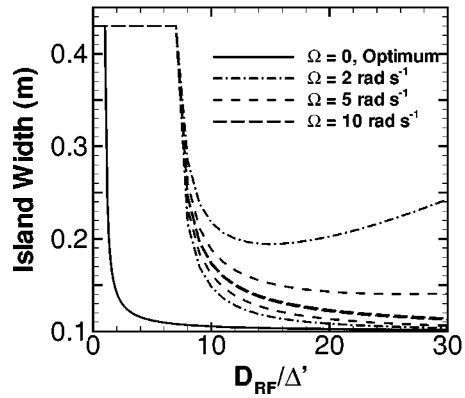

FIG. 8. Fast rotation in the presence of the auxiliary current leads to a stabilized island width comparable to static stabilization localized at the island O-point. Here, the results are based on an island evolution equation with $\alpha = 0.7$ and $\delta_j^2 + W_d^2 = 0.1$.

When W_d is less than half the current channel width, the minimum island width is determined by half the current channel width, otherwise it is set by W_d. This observation can be incorporated into a simple formula for $\Delta'_{\rm rf}$ that can be used in a standard island evolution equation and is motivated by the island evolution equation in Ref. 11. The result is

$$\Delta'_{\rm rf} = D_{\rm rf}\left(1 - \frac{(W_d^2 + \delta_J^2/4)}{W^2}\right), \qquad (8)$$

where $D_{\rm rf}$ is a constant coefficient proportional to the rf current source that is sufficiently large to stabilize the initial island width. For an island width that is initially much larger than either the current channel or the anisotropic diffusion width this requires that $D_{\rm rf} > \Delta'$. The saturated island then scales as

$$W_{\rm sat}^2 = \frac{(W_d^2 + 0.25\delta_J^2)}{1 - \dfrac{\Delta'}{D_{\rm rf}}}. \qquad (9)$$

Even if the current source is allowed to become large $D_{\rm rf} \to \infty$, the maximum stabilized island width is at best $W_{\rm sat}^2 = (W_d^2 + 0.25\delta_J^2)$.

One feature that is missing from this simple model, but which appears in the simulation, is the phase instability that occurs when the island width becomes sufficiently small and the island slips in phase slightly so that the X-point aligns with the peak of the auxiliary current. This effectively causes the sign of $D_{\rm rf}$ to change and become destabilizing. The passive stabilization scheme suggests that if the island is not allowed to lock to the peak of the auxiliary current but instead rotates continuously past the peak, then net stabilization is possible. To provide a cursory exploration of this passive stabilization scheme, a simplified island evolution equation is proposed, that is given by

$$\frac{\mu_0}{\eta}\frac{dW}{dt} = \Delta' + \Delta'_{\rm rf}(f - \alpha(1-f)), \qquad (10)$$

where α represents the decrease in efficiency for a current source located at the X-point relative to the O-point, and $f = 0.5 + 0.5\cos(\Omega t)$ is a factor that accounts for island rotation past the auxiliary source. A phase has been chosen that reverts to the original island equation with zero rotation. One of the caveats of this approximation is that the temporal dynamics of the finite diffusion effects may be over-simplified with respect to choosing a single coefficient α. The choice of α is based on the observation that the same current localized at the X-point causes somewhat less than a factor 2 increase in growth rate in the static case. Figure 8 illustrates that in the presence of rotation and for an $\alpha = 0.7$ and $W_d^2 + \delta_j^2/4 = 0.1$, at least a factor of 4 increase in auxiliary current relative to the case phased exactly at the O-point is required to cause stabilization. Furthermore, the island width oscillates between two amplitudes that coalesce towards one value as the rotation rate increases. The minimum island width does not fall below the level that has been chosen for $W_d^2 + \delta_j^2/4$.

IV. CONCLUSIONS

Numerical simulations of the stabilization of a resistive tearing mode by rf-induced current indicate that stabilization of the island is possible only down to a minimum island width, $W_{\min}$. Optimum stabilization is observed when the initial current source is localized at the island O-point. When the source offset is small relative to the island width, the effect of a misaligned current source is small. However, as the island width decreases during stabilization and becomes on the order of the source offset the effect of poor localization is expected to become dominant. A source offset on the order of half the minimum island width is nominally required to effectively lead to stabilization that is not limited by poor localization of the current source. For optimal localization and for a sufficiently strong rf driven current, the minimum island width is principally a function of the current channel half-width $\delta_J/2$ and the anisotropic current diffusion width W_d. The minimum saturated island width is limited to the larger of these two quantities or more accurately $W_{\rm sat}^2 = (W_d^2 + 0.25\delta_J^2)$.

One of the motivations for these simulations was the prospect of stabilizing the neoclassical tearing mode observed in the experiment and expected to be problematic in fusion devices. If the nonlinear threshold for the neoclassical tearing mode is set by the anisotropic thermal diffusion mechanism, the ability to drive an island smaller than this width is impossible and near continuous stabilization of the mode would be required rather than stabilization only when the mode appears. This impossibility is predicated on the notion that the parallel and perpendicular diffusion coefficients for the electron temperature (which drives the neoclassical tearing mode through the bootstrap current) are the same or larger than the same diffusion coefficients for the fast electrons (which are associated with the rf induced current.) However, the difference would require many orders of magnitude since $W_d \propto (\chi_\perp / \chi_\parallel)^{0.25}$ and this is unlikely. The anisotropic diffusion threshold is not the only nonlinear threshold mechanism associated with the neoclassical tearing mode, turbulence/magnetic stochasticity and also the neoclassical enhancement of the polarization current may set the limit. If the nonlinear threshold is set by magnetic stochasticity, the expectation from these results based on transport arguments is that the stabilization process would be similarly limited by the stochasticity. However, the larger nonlinear threshold associated with neoclassical enhancement of the polarization current, suggests such stabilization may be more tractable.

ACKNOWLEDGMENTS

The author would like to thank the NIMROD team for the development of the NIMROD code. The author would also like to thank Maxime Zabiego and Xavier Garbet of Center-EurAtom-Cadarache for useful discussions and various ideas about island dynamics at small island width. The author would also like to thank Scott Kruger of Scientific Applications International Corporation for useful discussions on the accuracy of anisotropic diffusion models.

This work was supported by the United States Department of Energy.

[1] Z. Chang, E. D. Fredrickson, J. D. Callen *et al.*, Nucl. Fusion **34**, 1309 (1994).
[2] Z. Chang, J. D. Callen, E. D. Fredrickson, R. V. Budny, C. C. Hegna, K. M. McGuire, M. C. Zarnstorff, and the TFTR team, Phys. Rev. Lett. **74**, 4663 (1995).
[3] E. Fredrickson, S. H. Batha, M. G. Bell *et al.*, *Plasma Physics and Controlled Nuclear Fusion Research 1994* (International Atomic Energy Agency, Vienna, 1994), Vol. I, p. 275.
[4] B. A. Carreras, B. V. Waddell, H. R. Hicks, and S. J. Lynch, Phys. Rev. A **18**, 2732 (1978).
[5] W. X. Qu and J. D. Callen, Nonlinear growth of a single neoclassical MHD tearing mode in a tokamak, U. W. Plasma Report 85-5, National Technical Information Service, Springfield, VA 22161; copies may be ordered from the National Technical Information Service, Springfield, VA 22161 (1985); see National Technical Information Service Document No. DE6008946.
[6] R. Carrera, R. D. Hazeltine, and M. Kotschenreuther, Phys. Fluids **29**, 899 (1986).
[7] C. C. Hegna and J. D. Callen, Phys. Fluids A **4**, 1855 (1992).
[8] O. Sauter, R. J. Lahaye, Z. Chang *et al.*, Phys. Plasmas **4**, 1654 (1997).
[9] H. Zohm, M. Maraschek, G. Pautasso *et al.*, Plasma Phys. Controlled Fusion **37**, A313 (1995).
[10] H. Zohm, Phys. Plasmas **4**, 3433 (1998).
[11] C. C. Hegna and J. D. Callen, Phys. Plasmas **6**, 2940 (1997).
[12] G. Giruzzi, M. Zabiego, T. A. Gianakon, X. Garbet, A. Carinalli, and S. Bernabei, Nucl. Fusion **29**, 101 (1999).
[13] A. H. Reiman, Phys. Fluids **26**, 1338 (1983).
[14] Y. Yoshika, S. Kinoshita, T. Kabayashi *et al.*, Nucl. Fusion **24**, 565 (1984).
[15] P. H. Rutherford, in *Course and Workshop in Basic Physical Processes of Toroidal Fusion Plasmas, Varenna, Italy, 1985* (CEC EUR 10418 EN, Brussels, 1986), Vol. II, p. 531.
[16] D. W. Ignat, P. H. Rutherford, and H. Hsuan, in *Course and Workshop on Applications of RF Waves to Tokamak Devices, Varenna, Italy, 1985* (CEC EUR 10333 EN, Brussels, 1986), p. 525.
[17] E. Lazzaro and G. Ramponi, Phys. Plasmas **3**, 978 (1996).
[18] P. H. Rutherford, in *From Particles to Plasmas*, edited by J. W. Van Dam (Addison-Wesley, Redwood City, CA, 1989), p. 249.
[19] H. Zohm, G. Gantenbeim, G. Giruzzi *et al.*, Nucl. Fusion **39**, 577 (1999).
[20] P. Rutherford, Phys. Fluids **16**, 1903 (1973).
[21] H. Zohm, D. A. Gates, H. R. Wilson, G. Gantenbein, O. Gruber, S. Gunter, M. Maraschek, A. W. Morris, M. Sokoll, D. Wagner, ASDEX Upgrade Team, and COMPASS-D Team, Plasma Phys. Controlled Fusion **39**, B237 (1997).
[22] Q. Yu, S. Gunter, G. Giruzzi, K. Lackner, and M. Zabiego, Phys. Plasmas **7**, 312 (2000).
[23] R. Fitzpatrick, Phys. Plasmas **2**, 825 (1995).
[24] E. Lazzaro and M. F. Nave, Phys. Fluids **31**, 1623 (1988).
[25] A. H. Glasser, C. R. Sovinec, R. A. Nebel *et al.*, Plasma Phys. Controlled Fusion **41**, A747 (1999).
[26] J. M. Finn and C. R. Sovinec, Phys. Plasmas **5**, 461 (1998).
[27] G. Giruzzi, Plasma Phys. Controlled Fusion **A35**, 123 (1993).
[28] J. Killeen, G. D. Kerbel, M. G. McCoy, and A. A. Mirin, *Computational Methods for Kinetic Models of Magnetically Confined Plasmas* (Springer-Verlag, New York, 1986).